

Original

In vitro chromosomal aberrations induced by various shapes of multi-walled carbon nanotubes (MWCNTs)

Toshiaki Sasaki¹, Masumi Asakura¹, Chigusa Ishioka¹, Tatsuya Kasai¹, Taku Katagiri¹ and Shoji Fukushima¹

¹Japan Bioassay Research Center, Japan Organization of Occupational Health and Safety

Abstract: Objectives: IARC has classified one type of multi-walled carbon nanotubes (MWCNTs), MWNT-7, as possibly carcinogenic to humans (Group 2B); however, other types of MWCNT were categorized as not classifiable as to their carcinogenicity to humans (Group 3). *In vitro* chromosomal aberration assays of MWNT-7 showed polyploid formation but not structural abnormalities. This study investigated the influence of the shape and size of MWCNT on *in vitro* induction of chromosomal aberrations. **Methods:** Microscopic analysis and viable cell counting were used to assay for chromosomal aberrations and cytotoxicity induced in a Chinese hamster lung cell line (CHL/IU) exposed to different MWCNTs. **Results:** Using scanning electron microscopy, seven MWCNTs were classified into three types: straight fibrous, curved fibrous, and tangled. The straight fibrous MWCNTs were the strongest inducers of polyploidy and the most cytotoxic among the three types of MWCNTs. The curved fibrous MWCNTs induced more polyploidy than the tangled MWCNTs, and the cytotoxicity of both types seemed to be a reflection of their induction of polyploidy. None of the seven MWCNTs induced structural chromosomal aberrations. **Conclusion:** The non-clastogenicity of the MWCNTs indicates that the MWCNTs may not interact directly with DNA. Since the straight fibrous MWCNTs, which exhibit a structure similar to asbestos, were the strongest inducers of polyploidy, MWCNT shape may be an important factor in induction of polyploidy. We hypothesize that CHL/IU cells endocytosed MWCNTs and formed endosomes with shapes corresponding to those of the endocytosed

MWCNTs, and that the long axis diameter of the endosome is important in the capability of MWCNTs to induce polyploidy.

(J Occup Health 2016; 58: 622-631)

doi: 10.1539/joh.16-0099-OA

Key words: Carbon nanotube, Cell line, Chromosome aberrations, Cytotoxicity, Genotoxicity, Polyploidy

In concert with the development of nanotechnology, nanomaterials with new shapes and functions have been developed. Nanomaterials are used for industrial products and products for general consumers. In particular, because of their excellent physicochemical characteristics, carbon nanotubes (CNTs) are used in a large number of products such as semiconductors, batteries, pharmaceutical products, and clothing. However, there is concern about the effect of CNTs on human health. Because of their extremely small size, nanoscale level materials can have optical, electronic, mechanical, and chemical properties that are dramatically different from those of their larger forms, and while the properties of nanomaterials can be of great benefit to industry and manufacturing, the effect of nanomaterials on human health is generally unknown. Moreover, the ridged, straight, fibrous types of multi-walled carbon nanotubes (MWCNTs) are similar to asbestos, raising concern that these MWCNTs may be carcinogenic in humans. Finally, MWCNTs easily become airborne and can remain suspended in the air for considerable lengths of time. Consequently, there is a risk of exposure to a relatively high concentration of MWCNT in workplaces and long-term exposure to low concentrations of MWCNT in the general environment.

The genotoxicity of various MWCNTs has been investigated using a variety of assays and genetic markers for screening for human health hazards. While Ames tests of MWCNTs are generally negative, the results of chromosomal assays are mixed; MWCNTs have tested positive in

Received April 14, 2016; Accepted August 19, 2016

Published online in J-STAGE October 7, 2016

Correspondence to: T. Sasaki, Japan Bioassay Research Center, Japan Organization of Occupational Health and Safety, 2445 Hirasawa, Hadano, Kanagawa 257-0015, Japan (e-mail: toshiaki-sasaki@jbrs.johs.go.jp)

micronucleus assays¹⁻⁴), sister chromatid exchange assays¹), and chromosomal structural abnormality⁴) and numerical abnormality⁴) assays, but there are also reports of negative results in micronucleus assays⁵) and chromosomal structural abnormality^{6,7}) and numerical abnormality²) assays.

We have developed an effective method to evaluate the genotoxicity of MWCNTs using cultured cells⁸). Using this method to evaluate the genotoxicity of one of the MWCNTs, MWNT-7, we found that exposure to MWNT-7 resulted in formation of polyploidy and multinucleated cells but did not cause structural chromosomal aberrations, micronucleus induction, or *hprt* mutagenicity. This result suggests that MWNT-7 genotoxicity may be caused by physical interference of MWNT-7 with biological processes during cytokinesis rather than by direct interaction of the MWNT-7 with DNA. We hypothesized that physical interference of cytokinesis in cells treated with MWNT-7 may depend on the shape and size of MWNT-7. To test this possibility, a chromosomal aberration assay using various shapes and sizes of MWCNTs was conducted.

Materials and Methods

Chemicals

Seven different MWCNTs (CTa, CTb, CTc, CTd, CTe, CTf, and CTg) were used for chromosomal aberration assays. CTa (MWNT-7) and CTb were obtained from Hodogaya Chemical Co. Ltd. (Tokyo, Japan); CTc, CTd, and CTg were obtained from Tokyo Chemical Industry Co. Ltd. (Tokyo, Japan); CTe was obtained from Showa Denko K.K. (Tokyo, Japan); and CTf was made by shattering CTe in an agate mortar. Eagle's MEM was purchased from GIBCO (Invitrogen Cell Culture, CA, USA), and calf serum was purchased from SAFC Biosciences (Kansas City, USA). Dimethyl sulfoxide (DMSO), which was used as a solvent, and Mitomycin C (MMC), which was used as a positive control, were purchased from Wako Pure Chemical Industries, Ltd. (Osaka, Japan).

Cells

A clonal sub-line derived from the lung of a newborn female Chinese hamster (CHL/IU) was donated by the National Institute of Health Sciences (Tokyo, Japan). The cells were cultured with Eagle's MEM supplemented with 10% heat-inactivated calf serum (culture medium) and grown in a monolayer. The modal chromosome number was 25, and the doubling time was approximately 15 h. The CHL/IU cell line is widely used for chromosomal aberration testing; these cells are sensitive to induction of chromosomal aberration by chemical substances⁹⁻¹¹) including insoluble particles and fibers^{7,8,12,13}).

Suspension and dispersion of MWCNT

Since MWCNTs are water-insoluble and are easily aggregated/agglomerated into micron-sized particles, test substances must be suspended in an appropriate solvent and dispersed to isolated particles by ultrasonication. Previously, we found that 0.5% DMSO in culture medium was a suitable solvent⁸). 0.5% DMSO displayed no cytotoxicity toward CHL/IU cells. An ultrasonic homogenizer (S-4000, 20 kHz, 600 W, Misonix, Inc. New York, USA) was used to ultrasonicate the suspensions of MWCNT in the DMSO/culture medium. Ultrasonication for 3 min was previously determined to be optimal for dispersion of MWCNT in the DMSO/culture medium⁸). The desired amount of MWCNT was weighed, and the highest dosing suspension was prepared by suspending the test substance with the appropriate volume of DMSO and culture medium, and ultrasonication for 3 min. The remaining suspensions were prepared by serial dilution of the most highly concentrated MWCNT suspension with DMSO/culture medium. The cells were treated within 5 min after preparation of the MWCNT suspensions.

Shape and size of MWCNT in the culture medium (SEM observation)

To observe the shape and size of MWCNTs in the DMSO/culture medium, medium with MWCNT was applied onto a 0.2- μ m pore size Isopore Track-Etched membrane filter (Millipore, Bedford, USA) and dried. After the filter was sputter-coated with Pt, MWCNTs were observed by a scanning electron microscope (SEM; SU-8000, Hitachi, Ltd., Tokyo, Japan). CTa, CTb, CTc, CTd: The length and width of the fibers were measured on enlarged photo prints by a curvimeter (the length of 200 fibers of each MWCNT was measured) and a scale loupe (the diameter of 100 fibers of each MWCNT was measured). CTe, CTf, CTg: The long and narrow axes of the particles were measured on enlarged photo prints by a scale loupe (100 particles of each MWCNT were measured).

Chromosomal aberration assay

One hundred thousand cells were seeded onto a 60-mm plastic culture dish and incubated in culture medium for 24 h; then, the medium was replaced with MWCNT-medium. DMSO at 0.5% served as a negative control and MMC at 0.032 μ g/ml as a positive control. The cells were exposed to MWCNTs at concentrations ranging from 0.31 to 5000 μ g/ml for 45 h; treatment concentrations of each MWCNT were determined on the basis of a preliminary chromosomal aberration assay and cytotoxicity measurement (data not shown). MWCNT-media was changed to normal culture medium and colcemid was added to a final concentration of 0.1 μ g/ml 3 h prior to chromosome preparation. After the end of culture, the cells were dissociated with a fixed volume of trypsin so-

lution to make a cell suspension. A portion of the cell suspension was used for cell counting for the cytotoxicity measurement, and the remaining cell suspension was used for chromosome preparation. Chromosome specimens were prepared by the standard air-drying method and stained with 2% Giemsa. Two culture dishes were used for chromosome slide preparation and cytotoxicity determination for each dose.

For chromosome analysis, all slides, including the positive and negative controls, were independently coded before microscopic analysis. The frequency of the cells with various types of structural aberrations including chromatid breaks, chromatid exchange, chromosome breaks, chromosome exchange, and chromosome fragmentations, except pulverization, for each dose in 200 well-spread metaphases (100 metaphases/culture) as well as cells with numerical aberrations (polyploidy) were scored.

For cytotoxicity measurement, cytotoxicity was assessed by counting Trypan Blue-stained cells; viable cells exclude the dye, whereas dead cells stain blue due to dye uptake. The relative cell growth (RCG) was obtained by dividing the number of viable cells after 48 h (45 h exposure to MWCNTs and three h in fresh culture medium) by that of the negative control.

Uptake of MWCNTs by CHL/IU Cells (SEM observation)

CHL/IU cells were exposed to MWCNTs at 2.5 (CTa) and 100 (CTd, CTe, and CTf) $\mu\text{g}/\text{ml}$ for 48 h, pre-fixed in 1% glutaraldehyde in phosphate-buffered saline (PBS), rinsed four times in the PBS, and dehydrated using increasing concentrations of ethanol. The ethanol was replaced with *tert*-butanol and the samples were subjected to critical point drying. Surface membranes were removed with adhesive tape, and the sample was sputter-coated with Pt. Cells and phagocytosed MWCNT were examined by SEM.

Statistical analysis

The data of the positive and negative controls was compared using Fisher's exact test. The data of the MWCNTs-treated groups and negative controls was compared using Fisher's exact test, and Bonferroni correction was performed for multiple testing of the dose-groups. P values of less than 0.05 were considered to be statistically significant.

Results

Shape and size of MWCNTs in the culture medium (SEM observation)

SEM images of MWCNTs in the culture medium are shown in Fig. 1, and characteristics of the MWCNTs are summarized in Table 1. SEM images revealed that the seven MWCNTs used in this study can be classified by their morphology into two groups; fibrous types (CTa,

CTb, CTc, and CTd) and tangled types (CTe, CTf, and CTg). Further, the fibrous types can be further classified into straight types (CTa and CTb) and not straight (curved) types (CTc and CTd). The fibrous types were not agglomerated but dispersed into single fibers in the DMSO/culture medium. The mean lengths of CTa, CTb, CTc, and CTd were 5.7, 3.6, 4.0, and 4.2 μm , respectively. The mean widths of CTa, CTb, CTc, and CTd were 91, 144, 65, and 63 nm, respectively. The tangled types formed tightly packed spherical aggregates. CTe spherical aggregates were connected with thin fibers; thus, clusters of aggregates were dispersed in the DMSO/culture medium. The mean long axis and mean narrow axis of CTe were 8.3 and 2.3 μm , respectively. CTf and CTg spherical aggregates were individually dispersed in the DMSO/culture medium. The CTf and CTg aggregates both had the mean long axes of 3.3 μm and mean narrow axes of 2.3 μm .

Chromosomal aberration assay

From the results of preliminary chromosomal aberration assays, none of the seven MWCNTs caused structural chromosomal aberrations, but five MWCNTs (CTa, CTb, CTc, CTd, and CTe) caused polyploidy (data not shown). For the five MWCNTs that caused polyploidy in the preliminary experiment, cells were exposed to doses ranging from 0.31 to 1700 $\mu\text{g}/\text{ml}$. For CTf and CTg, which did not cause polyploidy in the preliminary experiment, cells were exposed to doses ranging from 310 $\mu\text{g}/\text{ml}$, the highest concentration showing no cytotoxicity in the preliminary experiment, to 5000 $\mu\text{g}/\text{ml}$, which is the maximum concentration required by the OECD test guideline 473 (1997) for chromosomal aberration tests. The chromosomal aberration assays of all MWCNTs were conducted in compliance with regulatory guidelines.

Results of structural chromosomal aberrations and polyploidy induction of various MWCNTs with CHL/IU cells are shown in Table 1 and 2. None of the MWCNTs induced any type of structural chromosomal aberration when cells were exposed to these doses for 45 h. In contrast, five of seven MWCNTs significantly induced numerical chromosome aberrations, i.e., polyploidy, ($p < 0.05$). The minimum dose levels of MWCNTs that caused significant induction of polyploidy were CTa and CTb at 1.2 $\mu\text{g}/\text{ml}$, CTc at 21 $\mu\text{g}/\text{ml}$, CTd at 62 $\mu\text{g}/\text{ml}$, and CTe at 100 $\mu\text{g}/\text{ml}$. CTf and CTg did not cause a significant increase in polyploidy at any concentration up to 5000 $\mu\text{g}/\text{ml}$. Thus, the polyploidy inducing ability of the MWCNTs is CTa = CTb > CTc > CTd > CTe.

As shown in Table 2, the cell toxicity patterns of the MWCNTs can be roughly classified into three types. The viability of cells exposed to straight fibrous MWCNT (CTa and CTb) exhibited steep cytotoxicity at 4.9 to 78 $\mu\text{g}/\text{ml}$. At the highest dose, the RCG of CTa and CTb were 64% and 43%, respectively. The curved fibrous

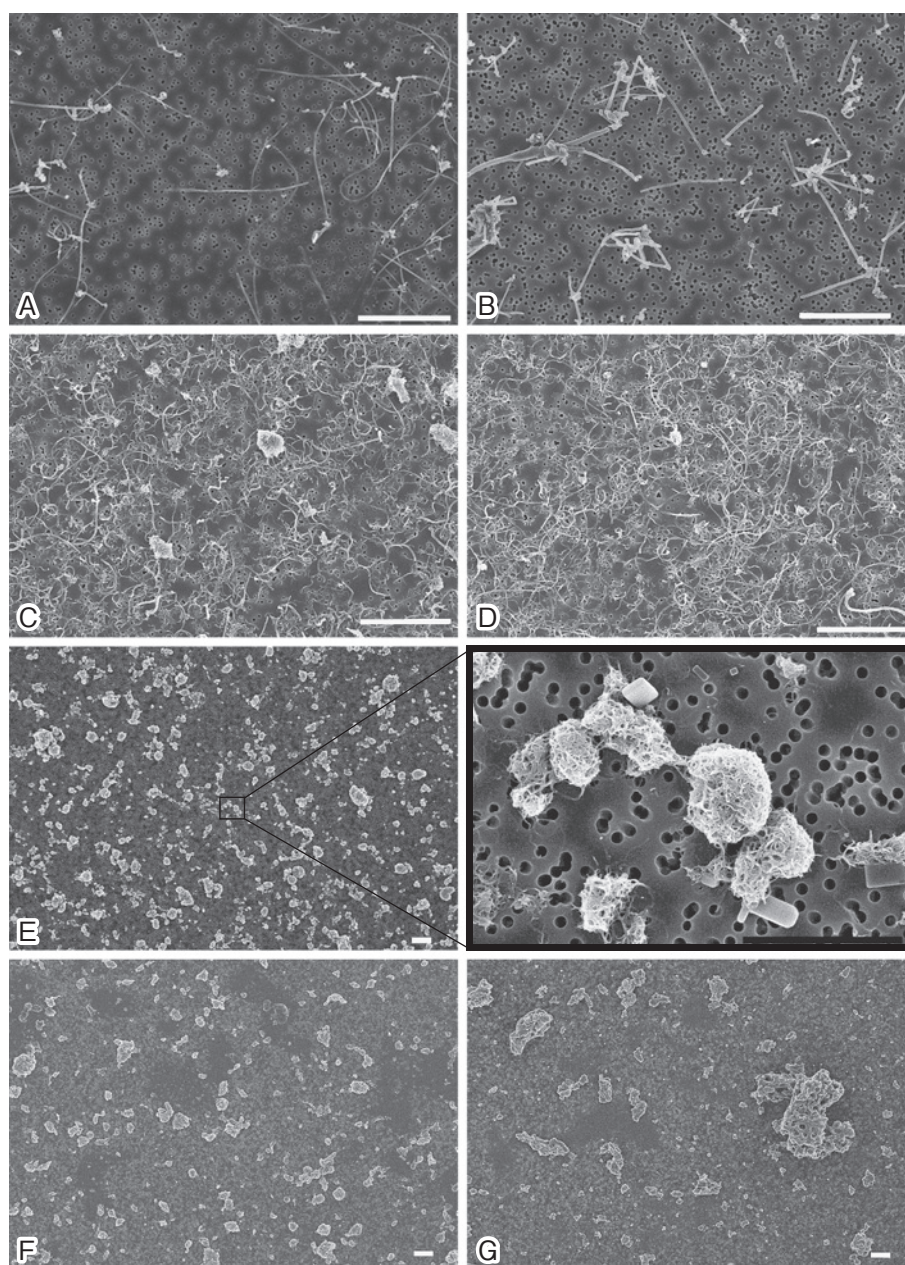


Fig. 1. An SEM image showing isolated fibers or tangles of MWCNTs in the medium. The white bar indicates 5 μm , and the black bar indicates 2 μm . Two straight fibrous types (A: CTa and B: CTb), two curved fibrous types (C: CTc and D: CTd), and three tangled types (E: CTe, F: CTf, and G: CTg) are shown. The concentrations of the MWCNT suspensions were CTa and CTb: 20 $\mu\text{g}/\text{ml}$; CTc, CTd, CTe, and CTg: 62 $\mu\text{g}/\text{ml}$; CTf: 40 $\mu\text{g}/\text{ml}$.

MWCNTs (CTc and CTd) were much less cytotoxic than the straight fibrous types and the cytotoxic effects were dose-dependent throughout the dose range (6.9-1700 $\mu\text{g}/\text{ml}$). At the highest dose, the RCG of CTc and CTd were 90% and 81%, respectively. The toxicity curves of the tangled types (CTe, CTf, and CTg) were mixed. The cytotoxic effects of CTe was similar to curved fibrous MWCNT and dose-dependent throughout the dose range

(25-300 $\mu\text{g}/\text{ml}$), while the viability of cells exposed to CTf and CTg exhibited steep cytotoxicity from 1300 to 5000 $\mu\text{g}/\text{ml}$ in a dose-dependent manner. At the highest doses, the RCG of CTe, CTf, and CTg were 91%, 38%, and 3%, respectively.

Uptake of MWCNTs by CHL/IU Cells (SEM observation)

Removal of the cell surface membrane using adhesive

Table 1. Summary of characteristics of MWCNTs and polyploidy induction

| | CTa ^{e)} | CTb | CTc | CTd | CTe | CTf | CTg |
|--|--------------------------------|--------------------------------|-------------------------------|-------------------------------|--------------------------------|---------------------------|-----------------------|
| Shape | fiber (straight) | fiber (straight) | fiber (curve) | fiber (curve) | tangle (cluster) | tangle (shattered CTe) | tangle (spherical) |
| Length (μm) ^{a)} | $5.7 \pm 3.6^f)$ | 3.6 ± 1.7 | 4.0 ± 3.8 | 4.2 ± 3.9 | 8.3 ± 5.2 | 3.3 ± 3.3 | 3.3 ± 3.1 |
| Width (nm) ^{b)} | $91 \pm 21^f)$ | 144 ± 25 | 65 ± 12 | 63 ± 12 | 2300 ± 2400 | 2300 ± 2400 | 2300 ± 2200 |
| Structural aberration ^{c)} | – | – | – | – | – | – | – |
| Polyploidy induction ^{d)} | + | + | + | + | + | – | – |
| | (1.2 $\mu\text{g}/\text{ml}$) | (1.2 $\mu\text{g}/\text{ml}$) | (21 $\mu\text{g}/\text{ml}$) | (62 $\mu\text{g}/\text{ml}$) | (100 $\mu\text{g}/\text{ml}$) | | |

^{a)} Fibrous types (CTa, CTb, CTc, CTd) showed fiber length, tangled types (CTe, CTf, CTg) showed long axis.

^{b)} Fibrous types (CTa, CTb, CTc, CTd) showed fiber width, tangled types (CTe, CTf, CTg) showed narrow axis

^{c)} Judgement of the structural chromosomal aberration induction

^{d)} Judgement of the polyploidy induction, and concentration expressed the minimal dose levels for the significant ($p < 0.05$) induction of polyploidy in parenthesis.

^{e)} Concentrations of the MWCNT suspension for length and width measurement: CTa and CTb: 20 $\mu\text{g}/\text{ml}$; CTc, CTd, CTe, and CTg: 62 $\mu\text{g}/\text{ml}$; CTf: 40 $\mu\text{g}/\text{ml}$

^{f)} Kasai T *et al.*, 2016¹⁸⁾

tape allowed the interior of the cell to be observed. SEM images of four types of MWCNTs localized in the cytoplasm of CHL/IU cells are shown in Fig. 2. The cell shown in Fig. 2A was exposed to 2.5 $\mu\text{g}/\text{ml}$ CTa (straight fibrous MWCNT): an internalized long straight fiber can be seen. The cell shown in Fig. 2B was exposed to 100 $\mu\text{g}/\text{ml}$ CTd (curved fibrous MWCNT); entangled fibers, similar to a bird's nest, can be seen in the cytoplasm. The cell shown in Fig. 2C was exposed to 100 $\mu\text{g}/\text{ml}$ CTe (tangled MWCNT); a large cluster of associated spherical aggregates can be seen in the cytoplasm. The cell shown in Fig. 2D was exposed to 100 $\mu\text{g}/\text{ml}$ CTf (shattered CTe); small aggregates scattered in the cytoplasm can be seen. Unlike the CTe aggregates, the CTf aggregates do not form large clusters.

Discussion

In this study, *in vitro* chromosomal aberration assays using seven different manufactured MWCNTs (including MWNT-7, CTa) were conducted. Examination of SEM images revealed that the seven MWCNTs could be categorized into three types, namely, straight fibrous, not straight (curved) fibrous, and tangled. The polyploidy inducing ability of the seven MWCNTs correlated to the three types of MWCNTs, but none of the seven MWCNTs caused structural chromosomal aberrations. Our results indicate that the shape of MWCNT fibers affects the capability of the fibers to induce polyploidy in CHL/IU cells.

As shown in Table 2, exposure to five of the seven MWCNTs investigated in this study caused polyploidy. Based on the minimum dose levels of MWCNTs that caused significant induction of polyploidy, the polyploidy inducing ability of the MWCNTs is CTa = CTb > CTc >

CTd > CTe, and CTf and CTg did not cause polyploidy. Thus, straight fibrous MWCNTs (CTa and CTb) were the strongest inducers of polyploidy, curved fibrous MWCNTs (CTc and CTd) were intermediated inducers of polyploidy, and the tangled MWCNT CTe was a weak inducer of polyploidy and the tangled MWCNTs CTf and CTg were not inducers of polyploidy. On the other hand, the fiber length or long axis diameter (LAD) of the MWCNT particles were CTe > CTa > CTd \geq CTc > CTb > CTf = CTg. Thus, an important factor for polyploidy inducibility may be the shape of the MWCNT rather than fiber length or LAD of the MWCNT particle.

Jensen *et al.*¹⁴⁾ showed that the inhibition of cytokinesis by long crocidolite asbestos fibers caused a significant increase in the incidence of polyploid cells (including binucleated and multinucleated cells) in a monkey kidney epithelial cell line. In addition, transmission electron microscopic observation by Jensen *et al.*¹⁴⁾ revealed that the asbestos fibers were enclosed within phagosomal membranes. Our SEM observation could not discriminate endosomal membranes, but MWCNTs seemed to be ingested via endocytotic vesicles of CHL/IU cells. As shown in Fig. 1A, isolated long straight fibers of CTa can be observed in an SEM image of a 20 $\mu\text{g}/\text{ml}$ CTa suspension. The CHL/IU cells, which were treated with 2.5 $\mu\text{g}/\text{ml}$ CTa, had long straight CTa fibers incorporated into the cytoplasm (Fig. 2A).

A model for cellular uptake of MWCNTs with different shapes is shown in Fig. 3. In panel 3A, we propose that an endocytosed CTa may be contained in an elongated vesicle with a larger LAD (also see Fig. 2A). Furthermore, we propose the elongated vesicles with larger LADs may interfere with cytokinesis in the cell, accounting for the strong induction of polyploidy by CTa. In favor of this proposal, Yasui *et al.*¹⁵⁾ showed that inhibition

Table 2. Structural aberration and polyploidy induction of MWCNTs with CHL/IU cells

| Treatment | Concentration ($\mu\text{g}/\text{ml}$) | Percentages (%) of structural aberration cells | | Percentages (%) of polyploidy cells | | Relative cell growth (%) |
|-------------------|--|---|------------------|--|------------|-----------------------------|
| | | Cell No. | CA ^{a)} | Cell No. | Polyploidy | |
| CTa | 0 | 200 | 0 | 203 | 1.5 | 100 |
| | 0.31 | 200 | 0 | 207 | 3.4 | 92 |
| | 1.2 | 200 | 0 | 216 | 7.4** | 91 |
| | 4.9 | 200 | 0 | 242 | 17.4** | 89 |
| | 20 | 200 | 0 | 285 | 29.8** | 82 |
| | 78 | 200 | 1.0 | 306 | 34.6** | 64 |
| MMC ^{b)} | 0.032 | 200 | 76.0** | 201 | 0.5 | – |
| CTb | 0 | 200 | 0.5 | 201 | 0.5 | 100 |
| | 0.31 | 200 | 0 | 203 | 1.5 | 88 |
| | 1.2 | 200 | 0 | 211 | 5.2* | 92 |
| | 4.9 | 200 | 0 | 223 | 10.3** | 94 |
| | 20 | 200 | 0.5 | 262 | 23.7** | 67 |
| | 78 | 200 | 0 | 300 | 33.3** | 43 |
| MMC ^{b)} | 0.032 | 200 | 42.0** | 200 | 0 | – |
| CTc | 0 | 200 | 0 | 202 | 1.0 | 100 |
| | 6.9 | 200 | 0 | 207 | 3.4 | 98 |
| | 21 | 200 | 0 | 213 | 6.1** | 96 |
| | 62 | 200 | 0.5 | 221 | 9.5** | 94 |
| | 190 | 200 | 0 | 226 | 11.5** | 91 |
| | 560 | 200 | 0.5 | 235 | 14.9** | 90 |
| MMC ^{b)} | 0.032 | 200 | 51.0** | 201 | 0.5 | – |
| CTd | 0 | 200 | 0 | 202 | 1.0 | 100 |
| | 6.9 | 200 | 0 | 204 | 2.0 | 101 |
| | 21 | 200 | 0 | 211 | 5.2 | 99 |
| | 62 | 200 | 0 | 214 | 6.5* | 97 |
| | 190 | 200 | 0 | 222 | 9.9** | 94 |
| | 560 | 200 | 0 | 232 | 13.8** | 90 |
| MMC ^{b)} | 0.032 | 200 | 47.5** | 200 | 0 | – |
| CTe | 0 | 200 | 0 | 201 | 0.5 | 100 |
| | 25 | 200 | 0 | 202 | 1.0 | 97 |
| | 50 | 200 | 0 | 208 | 3.8 | 97 |
| | 100 | 200 | 0 | 212 | 5.7** | 96 |
| | 200 | 200 | 0 | 219 | 8.7** | 93 |
| | 300 | 200 | 0 | 228 | 12.3** | 91 |
| MMC ^{b)} | 0.032 | 200 | 66.0** | 200 | 0 | – |
| CTf | 0 | 200 | 0.5 | 203 | 1.5 | 100 |
| | 310 | 200 | 0 | 205 | 2.4 | 100 |
| | 630 | 200 | 0.5 | 206 | 2.9 | 99 |
| | 1300 | 200 | 0.5 | 205 | 2.4 | 91 |
| | 2500 | 200 | 0 | 201 | 0.5 | 80 |
| | 5000 | 200 | 0 | 201 | 0.5 | 38 |
| MMC ^{b)} | 0.032 | 200 | 52.0** | 200 | 0 | – |
| CTg | 0 | 200 | 0.5 | 203 | 1.5 | 100 |
| | 310 | 200 | 1.0 | 204 | 2.0 | 100 |
| | 630 | 200 | 0 | 203 | 1.5 | 96 |
| | 1300 | 200 | 0 | 205 | 2.4 | 74 |
| | 2500 | 200 | 2.5 | 207 | 3.4 | 64 |
| | 5000 | TOX | | TOX | | 3 |
| MMC ^{b)} | 0.032 | 200 | 76.5** | 200 | 0 | – |

^{a)}CA: Structural chromosomal aberrations.

^{b)}MMC: Mitomycin C.

^{c)}Tox: Metaphase cells were not observed.

*Fisher's exact test: * $p < 0.05$, ** $p < 0.01$.

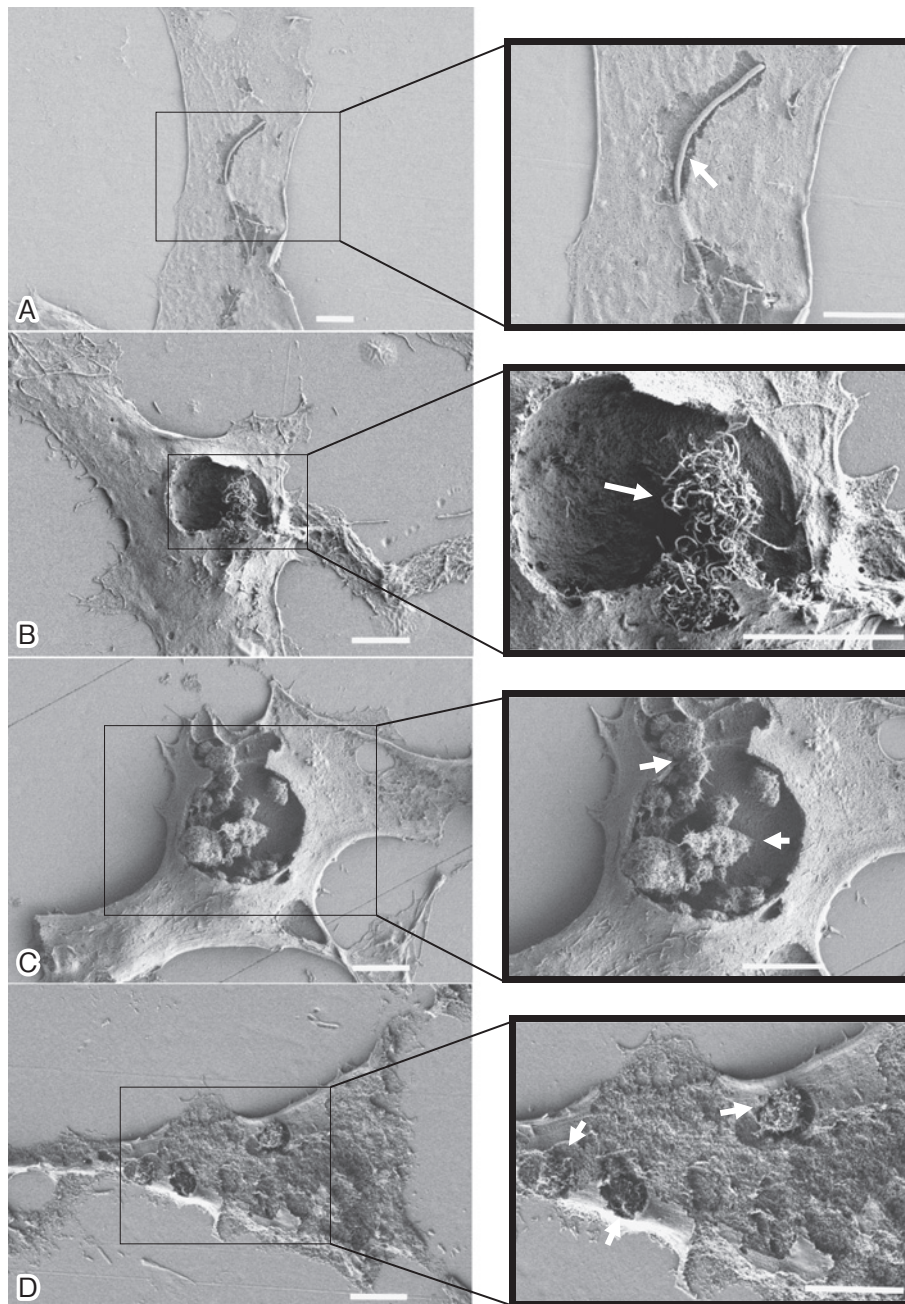


Fig. 2. Four types of MWCNTs localized in the cytoplasm of CHL/IU cells can be observed in cells with partially removed surface membranes areas. The cells were exposed to the four MWCNTs at 2.5 (CTa) and 100 (CTd, CTe, and CTf) $\mu\text{g}/\text{ml}$ for 48 h. A: An SEM image showing isolated long CTa fibers completely internalized into a CHL/IU cell. B: An SEM image showing entangled CTd fibers, similar to a bird's nest, internalized into a cell. C: An SEM image showing a large CTe cluster completely internalized into a cell. D: An SEM image showing small CTf aggregates scattered in the cytoplasm of a cell. The white bar indicates 5 μm . Arrows indicate internalized MWCNTs.

of cytokinesis by comparatively long MWCNT (MWNT-7) fibers during cell division induced the formation of polyploid cells (binucleated cells), whereas short MWCNTs did not induce polyploidy.

As shown in Fig. 1D, isolated and simple physically entangled fibers of curved CTd can be observed in an SEM image of a 62- $\mu\text{g}/\text{ml}$ CTd suspension. The cell shown in Fig. 2B was treated with 100 $\mu\text{g}/\text{ml}$ CTd and

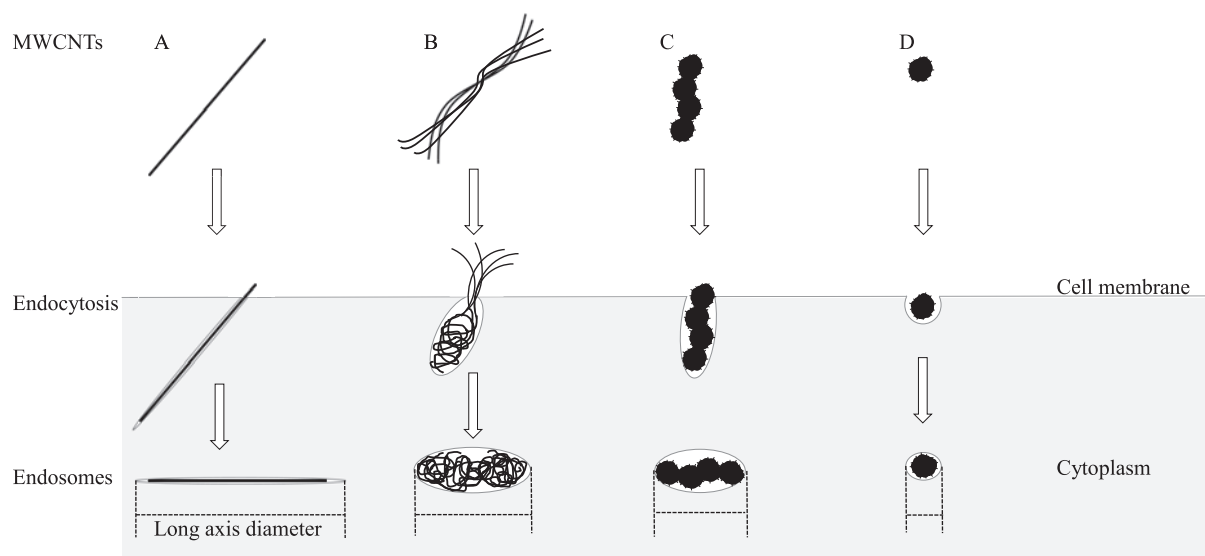


Fig. 3. A model for cellular uptake of MWCNTs with different shapes. A: Straight fibrous MWCNT; B: Curved fibrous MWCNT; C: Tangled MWCNT, a large cluster of associated spherical aggregates; D: Tangled MWCNT, small individual aggregates. The lengths of deformable curved fibrous MWCNT may be smaller after endocytosis than before endocytosis (B). The shape and size of non-deformable straight fibrous MWCNT (A) and tangled MWCNT (C, D) are not altered by endocytosis (see Fig. 2). Small tangled MWCNTs (D) are endocytosed into roughly spherical rather than elongated endosomes that do not effectively interfere with cytokinesis.

had entangled fibers, similar to a birds nest, in the cytoplasm. Since the deformable CTd may be distorted into a small mass by phagocytosis-related contractile activities in CHL/IU cells, the ends of these fibers seemed to be balled-up after endocytosis (Fig. 2B). Therefore, the LAD of the endosome containing the ingested CTd may be smaller than the CTd fiber length before endocytosis (Fig. 3B) and CTd was a weaker inducer of polyploidy than the straight fibrous CTa and CTb.

As shown in Fig. 1E, large and long clusters of associated spherical aggregates of tangled CTe can be observed in an SEM image of a 62- $\mu\text{g}/\text{ml}$ CTe suspension. The cell shown in Fig. 2C was treated with 100- $\mu\text{g}/\text{ml}$ CTe, and a typical CTe cluster of associated spherical aggregates can be seen localized in the cytoplasm. Endocytosed CTe are likely to be contained in large vesicles with large LADs, and the form of CTe does not appear to be altered by endocytosis (Fig. 2C, Fig. 3C). Since large endosomes containing the ingested CTe may interfere with cytokinesis in the cells, this would account for the induction of polyploidy by CTe.

As shown in Fig. 1F, small and short clusters of spherical aggregates of CTf are observed in an SEM image of a 40- $\mu\text{g}/\text{ml}$ CTf suspension. Since CTf was fabricated by shattering CTe in an agate mortar, CTf was smaller and shorter than CTe. The cell shown in Fig. 2D was treated with 100 $\mu\text{g}/\text{ml}$ CTf suspension, and small aggregates CTf could be observed scattered in the cytoplasm (Fig. 2D). CTf formed tightly packed aggregates that may

be non-deformable; thus, CTf is not altered by endocytosis (Fig. 2D, Fig. 3D). The small endosomes containing the ingested CTf may not interfere with cytokinesis in the cells, and this would account for the result that CTf did not induce polyploidy.

The discussion above suggests that straight fibrous CTa and CTb should be more potent inducers of polyploidy than deformable curved fibrous CTc and CTd, and that small tangled aggregates CTf and CTg should not induce polyploidy. However, the discussion also suggests that CTe, which is internalized into the largest endosome (LAD: approximately 8 μm), should be the most potent inducer of polyploidy, but CTe appears to exhibit a lower capability of inducing polyploidy than those of the straight and curved fibrous MWCNTs. This is because the lower capability of CTe to induce polyploidy is based on total mass ($\mu\text{g}/\text{ml}$) rather than on particle count. The sizes of CTa and CTe particles are 5700 \times 91 nm and 8300 \times 2300 nm, respectively. Thus, based on the size of the particles, the particle mass of CTe is 700-900 fold greater than that of CTa. Since the minimal dose levels of CTa and CTe that significantly increased the number of polyploid cells were 1.2 $\mu\text{g}/\text{ml}$ and 100 $\mu\text{g}/\text{ml}$, respectively, the capability of CTe to induce polyploidy was greater than that of CTa. Taken altogether, our results support the hypothesis that CHL/IU cells endocytosed MWCNTs and formed endosomes with shapes corresponding to the endocytosed MWCNTs and that the LAD of these endosomes is an important factor in the polyploidy inducing

capability of MWCNTs.

The cytotoxicity at lower MWCNT doses (0.31-630 µg/ml) corresponds to the shape of the MWCNTs: straight fibrous MWCNTs (CTa, CTb) > curved fibrous MWCNT (CTc, CTd) = tangled MWCNT (CTe) > tangled MWCNT (CTf, CTg). Thus, the cytotoxicity at lower MWCNT doses paralleled the capability of the MWCNTs to induce polyploidy. This result suggests that interfering with cytokinesis and consequently inhibiting cell proliferation was an important factor in MWCNT-mediated decreased RCG at lower doses of these MWCNTs. However, since CTf and CTg did not induce polyploidy and did not interfere with cytokinesis, there are likely to be cytotoxic mechanisms other than cytokinesis inhibition at higher doses of these MWCNTs.

There are two other chromosomal aberration studies of MWCNTs available. Ema *et al.*⁷⁾ reported that MWNT-7 and another straight-type MWCNTs increased the number of numerical chromosomal aberrations but did not increase the number of structural aberrations in CHL/IU cells. Our results that straight fibrous MWCNTs induced polyploidy but did not induce structural aberrations are in agreement with Ema *et al.*⁷⁾ Wirnitzer *et al.*⁶⁾ reported that tangled-type MWCNT particles did not increase the number of structural aberrations in V79 cells. Our results that tangled-type MWCNTs did not increase the number of structural aberrations are in agreement with those of Wirnitzer *et al.*⁶⁾ We previously reported that the *in vitro* genotoxicity of MWNT-7 was characterized by negative *hprt* mutagenicity, insignificant induction of micronuclei, the formation of polyploidy without structural chromosomal aberrations, and increased numbers of binucleated and multi-nucleated cells and proposed that MWNT-7 interfered physically with biological processes during cytokinesis but did not directly interact with the DNA⁸⁾. The results of the present study extend our previous findings by suggesting that physical interference with cytokinesis depends on the shape of the MWCNT fibers.

Nagai *et al.*^{16,17)} reported that in one intraperitoneal injection study, MWNT-7 and two other straight-type MWCNTs caused mesotheliomas in male and female rats but one tangled type of MWCNT 15 nm in diameter did not. Our results that fibrous straight MWCNTs induced polyploidy and tangled MWCNTs 3.3 × 2.3 µm in size did not suggest the possibility that polyploid cells may have been one of the causes of cancer in the studies by Nagai *et al.*^{16,17)}.

In a two-year, whole-body inhalation study, MWNT-7 (CTa in the present study, a straight fibrous MWCNT) caused lung cancer in rats¹⁸⁾. IARC classified MWNT-7 as possibly carcinogenic to humans (Group 2B), but other MWCNTs were classified as not classifiable as to their carcinogenicity to humans (Group 3)¹⁹⁾. However, the capability of the MWCNT designated CTb in the present study, another straight fibrous MWCNT, to induce poly-

ploidy is almost equivalent to MWNT-7. Thus, it is necessary to perform carcinogenicity studies of other straight fibrous MWCNTs. Moreover, to identify shapes of MWCNTs that are probably not carcinogenic to humans, it is necessary to perform carcinogenicity studies of curved fibrous MWCNTs and tangled MWCNTs.

Conclusion

Non-clastogenicity of MWCNTs indicates that seven MWCNTs may not interact directly with DNA. Since the straight fibrous MWCNTs, having a structure similar to asbestos, were the strongest inducers of polyploidy, MWCNT shape may be an important factor in MWCNT induction of polyploidy. We hypothesize that CHL/IU cells ingested MWCNTs and formed endosomes with shapes corresponding to those of ingested MWCNTs, and that the long axis diameter (LAD) of the endosome is an important factor in the capability of MWCNTs to induce polyploidy.

Acknowledgments: The authors acknowledge the technical support from Mr. Masahiro Yamamoto. The present study was contracted and supported by the Ministry of Health, Labour and Welfare of Japan.

Conflicts of interest: The authors declare that they have no conflicts of interest.

References

- 1) Kato T, Totsuka Y, Ishino K, et al. Genotoxicity of multi-walled carbon nanotubes in both *in vitro* and *in vivo* assay systems. *Nanotoxicology* 2013; 7: 452-461.
- 2) Migliore L, Saracino D, Bonelli A, et al. Carbon Nanotubes Induce Oxidative DNA Damage in RAW 264.7 Cells. *Environ Mol Mutagen* 2010; 51: 294-303.
- 3) Cveticanin J, Joksic G, Leskovic A, Petrovic S, Sobot AV, Neskovic O. Using carbon nanotubes to induce micronuclei and double strand breaks of the DNA in human cells. *Nanotechnology* 2010; 21: 015102.
- 4) Di Giorgio ML, Di Bucchianico S, Ragnelli AM, Aimola P, Santucci S, Poma A. Effects of single and multi walled carbon nanotubes on macrophages: cyto and genotoxicity and electron microscopy. *Mutat Res* 2011; 722: 20-31.
- 5) Ponti J, Broggi F, Mariani V, et al. Morphological transformation induced by multiwall carbon nanotubes on Balb/3T3 cell model as an *in vitro* end point of carcinogenic potential. *Nanotoxicology* 2013; 7: 221-233.
- 6) Wirnitzer U, Herbold B, Voetz M, Ragot J. Studies on the *in vitro* genotoxicity of baytubes, agglomerates of engineered multi-walled carbon-nanotubes (MWCNT). *Toxicol Lett* 2009; 186: 160-165.
- 7) Ema M, Imamura T, Suzuki H, Kobayashi N, Naya M, Nakanishi J. Evaluation of genotoxicity of multi-walled carbon nanotubes in a battery of *in vitro* and *in vivo* assays. *Regul Toxicol*

- Pharmacol 2012; 63: 188-195.
- 8) Asakura M, Sasaki T, Sugiyama T, et al. Genotoxicity and Cytotoxicity of Multi-wall Carbon Nanotubes in Cultured Chinese Hamster Lung Cells in Comparison with Chrysotile A Fibers. *J Occup Health* 2010; 52: 155-166.
 - 9) Ishidate M Jr, Miura KF, Sofuni T. Chromosome aberration assays in genetic toxicology testing in vitro. *Mutat Res* 1998; 404: 167-172.
 - 10) Ishidate M Jr, Odashima S. Chromosome tests with 134 compounds on Chinese hamster cells in vitro—a screening for chemical carcinogens. *Mutat Res* 1977; 48: 337-353.
 - 11) Organisation for Economic Co-operation and Development (OECD). OECD guideline for the testing of chemicals 473: in vitro mammalian chromosomal aberration test. [Online]. 2014 [cited 2016 Oct. 12]; Available from: URL: http://www.oecd-ilibrary.org/environment/test-no-473-in-vitro-mammalian-chromosomal-aberration-test_9789264224223-en
 - 12) Kawaguchi Y, Hayashi H, Sato M, Shindo Y. Needle crystals of vitamin B₂ induce polyploidy in Chinese hamster lung (CHL/IU) cells. *Mutat Res* 1997; 373: 1-7.
 - 13) Matsuoka A, Onfelt A, Matsuda Y, et al. Development of an *in vitro* screening method for safety evaluation of nanomaterials. *Biomed Mater Eng* 2009; 19: 19-27.
 - 14) Jensen CG, Jensen LC, Rieder CL, Cole RW, Ault JG. Long crocidolite asbestos fibers cause polyploidy by sterically blocking cytokinesis. *Carcinogenesis* 1996; 17: 2013-2021.
 - 15) Yasui M, Kamoshita N, Nishimura T, Honma M. Mechanism of induction of binucleated cells by multiwalled carbon nanotubes as revealed by live-cell imaging analysis. *Genes Environ* 2015; 37: 6.
 - 16) Nagai H, Okazaki Y, Chew SH, et al. Diameter and rigidity of multiwalled carbon nanotubes are critical factors in mesothelial injury and carcinogenesis. *Proc Natl Acad Sci U S A* 2011; 108: E1330-1338.
 - 17) Nagai H, Okazaki Y, Chew SH, et al. Intraperitoneal administration of tangled multiwalled carbon nanotubes of 15 nm in diameter does not induce mesothelial carcinogenesis in rats. *Pathol Int* 2013; 63: 457-462.
 - 18) Kasai T, Umeda Y, Ohnishi M, et al. Lung carcinogenicity of inhaled multi-walled carbon nanotube in rats. *Part Fibre Toxicol* 2016; 13: 53.
 - 19) Grosse Y, Loomis D, Guyton KZ, et al. Carcinogenicity of fluoro-edenite, silicon carbide fibres and whiskers, and carbon nanotubes. *Lancet Oncol* 2014; 15: 1427-1428.